Robust Estimator Design for Control of Electropneumatic System

Lilia Sidhom, Mohamed Smaoui, Xavier Brun, Eric Bideaux

Robust estimator design for control of electropneumatic system

Journal:	*IETE Journal of Research*
Manuscript ID	Draft
Manuscript Type:	Original Article
Date Submitted by the Author:	n/a
Complete List of Authors:	SIDHOM, LILIA; ENIT , SMAOUI, Mohamed; INSA Lyon brun, xavier; INSA Lyon bideaux, eric; INSA Lyon
Keywords:	Estimator/Controller design, higher order sliding modes, experimentation, electropneumatic system
Abstract:	In this paper, hybrid position/force controller is considered for high dynamic electro-hydraulic servo-actuator. The purpose is to apply specified force to flexible load after a moving to some position. This cycle can be repeated several times with different magnitude and frequencies of force and position. The main advantage of such strategy law consists principally to the industrial fatigue test application, but some dangerous damages could occur especially at switching times. Our contribution consist to propose a method to generate automatically the switching signal in order to commute between the two controllers with any abrupt change of state, despite the presence of uncontrolled dynamics. To show the effectiveness of the proposed approach, simulation results on the electro-hydraulic system are carried out.

Robust estimator design for control of electropneumatic system

L. Sidhom [1], M. Smaoui [2], X. Brun [2] and E. Bideaux [2]

[1]Research Laboratory LA.R.A, ENIT, BP 37, Le Belvédère, Tunis, 1002 Tunisia; (e-mail: lilia.sidhom@gmail.com).
[2] AMPERE Laboratory UMR 5005, INSA of Lyon, 20 Avenue Albert Einstein, Villeurbanne, Lyon, F 69621, France

ABSTRACT
In this paper, hybrid position/force controller is considered for high dynamic electro-hydraulic servo-actuator. The purpose is to apply specified force to flexible load after a moving to some position. This cycle can be repeated several times with different magnitude and frequencies of force and position. The main advantage of such strategy law consists principally to the industrial fatigue test application, but some dangerous damages could occur especially at switching times. Our contribution consist to propose a method to generate automatically the switching signal in order to commute between the two controllers with any abrupt change of state, despite the presence of uncontrolled dynamics. To show the effectiveness of the proposed approach, simulation results on the electro-hydraulic system are carried out.

Keywords:
Estimator/Controller design; higher order sliding modes; experimentation; electropneumatic system.

1. INTRODUCTION

Pneumatic actuators are widely used in several industrial applications. These kinds of systems have the potential to provide high output power to weight and size ratios at a relatively low cost. However, the complexity of the electropneumatic systems and the wide range of control laws are real industrial problems where the aim is to choose the best control strategy for a given application. These last decades, numerous research works have been focused to meet this requirement. Most of them have been in the field of feedback linearization [1], [2]. Other investigations have been conducted on adaptive control [3], Backstepping control [4] and high order sliding modes control [5], [6]. All of these controllers require in general measurements of velocity and acceleration for feedback. For example, the acceleration measure can improve the performance of some flexible mechanical system such as the motion control of servo drives. Although the acceleration feedback is sometimes necessary to ameliorate performance of drive systems, this state variable is seldom measured in practical case owed to the unsatisfactory results of many existing methods. These last usually produce inaccurate, delayed or noisy acceleration estimates. Moreover, the employment of such physical sensors to measure speed and acceleration can adds cost and energy consumption and it also increases the complexity of the system.
So the aim of our research work consists to avoid these difficulties in order to minimize the sensors number on some test-bench. In fact, a proposed estimator scheme is used to estimate in parallel the first and the second derivative of a measured position signal which is addressed to a control-loop problem.

For dealing with the real-time estimation problem, in the literature several solutions are already proposed. One of basic solution is the finite difference method such as the Euler backward differentiation formula. This last one is simple to implement and it is the most common numerical method that can be applied in real time. Unfortunately this method provides noise to an unacceptable level on the estimates. Although this problem is deleted with using a low-pass filter, a harmful delay can be inevitable. Other methods are based on digital filter differentiators which can be designed by targeting some design purposes. In [19], the authors present a method that is based on a polynomial predictive filtering. This method has two drawbacks. On the one hand, some features of the signal and the noise must be considered to build such scheme. On the other hand, a long delay-line is required for the filter hardware implementations. Other approaches consist of casting the differentiation problem with using observer-based methods. Therefore, the knowledge of the system/noise model is necessary which is disadvantage of such method. For the nonlinear observer theory, the used model is generally not much representative to the physical system then obtained results are not too significant. Other robustness approaches exist to compensate the model uncertainties such as sliding mode observers [20], [21], but generally there are always assumptions imposed on the uncertainties.

The use of numerical differentiation schemes enables a model-independent derivation is an alternative approach. Then, in contrast to Kalman filter, the chosen derivative estimation technique must not require the stochastic features or/and model knowledge of the both process and/or noise. Therefore, the differentiation problem becomes more trivial when the noise properties are not very well-known or may change with time. Recently, numerous differentiator schemes have been

proposed. The main difficulty here is to find a suitable differentiator scheme able to reduce the effect of noise while trying to leave the informative signal unchanged and without delay. In fact, practical differentiation is a trade-off between the exact differentiation and the noise rejection. Where the structure of the signal may be unknown except for some differential inequalities, differentiators that are based on algebraic parametric estimation techniques can be well employed [22], [23]. Indeed, the authors have calculated estimation of time derivative of an analytic function using the truncated series of Taylor expansion. After some computation done in operational domain, a system of linear equation is obtained leads to giving the estimated values of derivatives. Although the algebraic algorithms allow a good capability to attenuate efficiently the noise, they are sensitive to the truncation order also to the size of the sliding window estimation and essentially to the setting of its parameters. Alternative methods based on the higher order sliding mode technique can be used [7]. In [8], a robust first-order sliding modes differentiator called Super Twisting is proposed to estimate the first order derivative of a bounded noisy signal. In [10], the author generalises the Super-Twisting differentiator to an arbitrary-order derivative of a bounded noisy signal, with finite-time convergence. The main advantages of such differentiators are the easiness of its implementation in real time. That is why; numerous applications have been successfully performed with using sliding modes differentiators specifically the first order. For instance, in [9] the authors used the Super-Twisting algorithm in a context of control objective where the setting of its gains was made manually. Even though large applications of these kinds of differentiators have been performed, its major drawback concerns the tuning of its gains in real time. This adjustment requires the exactly knowledge beforehand of the Lipschitz constant of the derivative signal. Furthermore, it is very difficult to obtain in advance the value of this constant in real time since we do not necessarily know the signal to estimate. In the prior researches, different new schemes of sliding modes differentiators have been proposed to improve the performance of basic schemes and also to avoid their problem of parameter adjustment. Some works that can be cited are: [17], [18]. In these last, a new forms of the first-order differentiator are proposed and where they have been applied with satisfactory results.

In the current paper, we are going to develop the results from [10] in order to propose novel scheme of second-order differentiator which is based on third-order sliding mode. As per the author's best knowledge, the proposed algorithm is used perhaps for the first time for position control of an electro-pneumatic actuator. In this paper, we introduce original dynamic gains to adjust them in real time and to avoid the condition of the Lipschitz constant of Levant's differentiator. Moreover, in all the previous works, generally, all contributions that have been made relate to the first order estimator which is based on the second order sliding mode. Indeed, our contributions consist to propose unit estimator which it can compute simultaneous the speed and the acceleration and its integration into a control-loop of electro-pneumatic system instead of physical sensors.

The outline of this paper is as follows. In section 2, the generalized problem formulation for higher order sliding modes time derivative estimation is explained. Thereafter, the proposed algorithm is presented. To show the effectiveness of the new scheme, some experiment was carried out using the electro-pneumatic system. So in section 3, the model of this system is presented. In section 4, some experimental results are performed in control-loop context where discussion of these results is then given.

2. DERIVATIVES ESTIMATION BASED ON SLIDING MODES

As well as for the robust controller's design, the higher order sliding modes technique shows also good results in the synthesis of robust differentiators [7], such as the Super Twisting (ST) algorithm [9]. For an estimate of an order derivative higher than one, derivative estimation problem can also be solved by the arbitrary-order robust differentiator proposed by Levant [7]. In this paper, a 2nd-order Robust Differentiator (RD) with finite time convergence given in [7] is studied.

2.1 Problem Statement

Consider an input signal of differentiator $f(t)$ as a function defined on $[0,\infty[$ measurable in Lebesgue's sense which can be considered as the sum of two following terms:

$$f(t) = f_0(t) + \xi(t) \tag{1}$$

$f_0(t)$ is an unknown clear-off-noise signal with the *(n+1)*th derivative having a known Lipschitz constant $C > 0$. $\xi(t)$ is a bounded Lebesgue-measurable noise with unknown features and it is defined by: $|\xi(t)| < \varepsilon$, with ε is sufficiently small so $|f(t) - f_0(t)| \le \varepsilon$.

The recursive diagram of differentiator proposed in [9] aims to obtain a robust estimate in real time of $\dot{f}_0(t), \ddot{f}_0(t), ..., f_0^{(n)}(t)$ being exact in absence of the noise. The task here is to find derivative estimates using only values of $f(t)$ and the value constant C. The 2nd-order RD is defined by the following equations:

$$\begin{cases} \dot{z}_0 = v_0; v_0 = -\lambda_0 |z_0 - f|^{\frac{2}{3}} sign(z_0 - f) + z_1, \\ \dot{z}_1 = v_1; v_1 = -\lambda_1 |z_1 - v_0|^{\frac{1}{2}} sign(z_1 - v_0) + z_2, \dot{z} \\ \dot{z}_2 = -\lambda_2 sign(z_2 - v_1) \end{cases} \tag{2}$$

Where $\lambda_0, \lambda_1, \lambda_2$ are differentiator parameters which must be positive values depending on the constant Lipschitz C of $\ddot{f}_0(t)$ and v_0, v_1 are the outputs of the differentiator.
Initializing (time t=0) this algorithm can well be performed as follows $z_0(0) = f(0)$, $z_1(0) = z_2(0) = 0$. So after a finite time and in absence of noise, we obtain $z_1 = v_0$ is the estimation of $\dot{f}_0(t)$ whereas $z_2 = v_1$ is the estimation of $\ddot{f}_0(t)$.
Some explications must be needed before presenting the proposed scheme. So, return to the system (2), remark that from the last equation of this system, the following equality is hold:

$$\dot{z}_2 = -\lambda_2 sign(z_2 - v_1) = -\lambda_2 sign(z_1 - v_0) \quad (3)$$

In effect, from the fourth equation of the previous system, we have:

$$z_2 - v_1 = \lambda_1 |z_1 - v_0|^{\frac{1}{2}} sign(z_1 - v_0) \quad (4)$$

In view of this inequality $\lambda_1 |z_1 - v_0|^{\frac{1}{2}} \geq 0$, the following expression can be assured $sign(z_2 - v_1) = sign(z_1 - v_0)$.
Note that the two last equations of this system can be rewritten in this following form:

$$\begin{cases} v_1 = -\lambda_1 |z_1 - v_0|^{\frac{1}{2}} sign(z_1 - v_0) + \lambda_2 z_2 \\ z_2 = -sign(z_1 - v_0) \end{cases} \quad (5)$$

This is explained by the fact that the gain λ_2 is a constant value. Thereafter, this transformation will be used to design the novel scheme of 2nd-order RD given in the next section.
According to the Levant's condition [10], the parameters $\lambda_i, i \in \{0,1,2\}$ can be chosen by using the following expression:

$$\lambda_i = \lambda_{i0} C^{\frac{1}{2-i+1}} \quad (6)$$

Where the gains λ_{i0}, $i \in \{0,1,2\}$ are positive.
From eq.6, the gains values can be computed by taking into account the maximum frequency component and maximum amplitude of the input signal $f(t)$. This condition (eq. (6)) gives some idea to tune the parameters algorithm but the best way in the practical case rests to guess them by computer simulation. Moreover, for some bandwidth of the input signal, it is not so easy to tune them due to their dependence on the value of the Lipschitz Constant C. Therefore; each modification of the spectral content of the input signal or of its magnitude affect significantly the quality of the estimated signals.
To get an idea of the gain values effect on the estimator accuracy, two simulation tests are carried. For the 1st test, the considered input signal is a sinusoidal one and defined by $f(t) = \sin(2t)$ with its pulsation ω is equal to $\omega = 2rad/s$. Obviously, for a such signal, the Lipschitz constant is given by $C = \omega A$, where A is the signal magnitude and ω its pulsation. Then, in the 2nd test the parameter values of the estimator are keeping the same with increasing the Lipschitz constant of the signal $f(t)$ by changed up its pulsation to $4rad/s$.

To illustrate the adjustment problem of RD, the errors curves for each outputs of RD are respectively given in figures 1 and 2 with considering different pulsation of the input signal and the same gain values. These gain values they are properly selected in relation to the Lipchitz condition of the input signal relative to $\omega = 2rad/s$. In figures 1 and 2, the errors represent the difference between the estimated signal by the RD estimator and the analytical derivative. These figures assert that even slight changes of the input signal pulsation make degraded algorithm accuracy. For greater precision, the figure 1 shows that for the estimation of the 1st derivative, the error for the 2nd test is about 19 times more important than this given by the 1st one. For the 2nd derivative estimation, the error of the 2nd test becomes so higher than the 1st test.

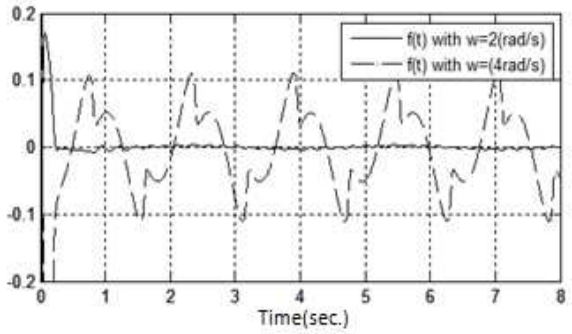

Figure 1. Error evolution for the 1st derivative estimate.

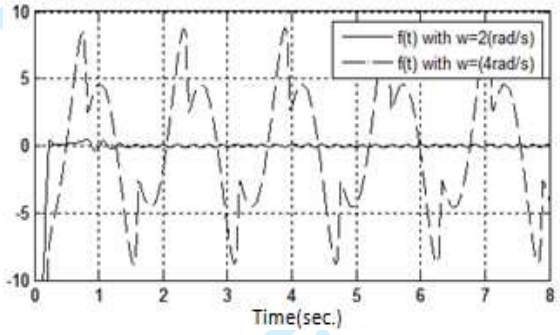

Figure 2. Error evolution for the 2nd derivative estimate.

Therefore, the parameterization of the sliding modes estimator (RD) depends on the input signal is an effective limit of the method performances. Then, the algorithm gains must be chosen judiciously to differentiate in real time some input signal which has rich frequency spectrum. Remark that in the presence of the noise, the gain values must not be chosen too large in order not to differentiate the noise.

This problem can be resolved by making the estimator gains having some dynamic laws with respect to the measured signal variations. The proposed solution is exposed in the next subsection where the new scheme of the RD is explained.

2.2 Proposed Differentiation Algorithm

Let's define the Proposed Differentiator (PD) given by the following system:

$$\begin{cases} \dot{z}_0 = v_0; \;\; v_0 = -\hat{\lambda}_0 |s_0|^{\frac{2}{3}} sign(s_0) + z_1 - K_0 s_0 \\ \dot{z}_1 = v_1; \;\; v_1 = -\hat{\lambda}_1 |s_1|^{\frac{1}{2}} sign(s_1) - \hat{\lambda}_2 \int_0^t sign(s_1)\, dt - K_1 s_1 \end{cases} \quad (7)$$

$\hat{\lambda}_0, \hat{\lambda}_1, \hat{\lambda}_2$ are dynamic gains, K_0 and K_1 convergence gains and s_0, s_1 the sliding surfaces defined as:

$$\begin{cases} s_0 = z_0 - f \\ s_1 = z_1 - v_0 \end{cases} \quad (8)$$

The dynamic gains $\hat{\lambda}_i, i \in \{0,1,2\}$ are defined by:

$$\begin{cases} \dot{\hat{\lambda}}_0 = \left[|s_0|^{\frac{2}{3}} sign(s_0) \right] s_0, \;\; \hat{\lambda}_0(0) \geq 0 \;\; and \;\; \hat{\lambda}_0 > 0 \;\; \forall t > 0 \\ \dot{\hat{\lambda}}_1 = \left[|s_1|^{\frac{1}{2}} sign(s_1) \right] s_1, \;\; \hat{\lambda}_1(0) \geq 0 \;\; and \;\; \hat{\lambda}_1 > 0 \;\; \forall t > 0 \\ \dot{\hat{\lambda}}_2 = s_1 \int_0^t sign(s_1)\, dt \end{cases} \quad (9)$$

Theorem 1. *For $K_0, K_1 > 0$ and with the dynamic gains $\hat{\lambda}_i, i \in \{0,1,2\}$ defined by (9), the system trajectories (7) converge locally and asymptotically towards the equilibrium point $s_0 = s_1 = 0$ under the assumption that as there are a positive constants λ_0^*, λ_1^* and λ_2^*, a priori unknown, defined by:*

$$\begin{cases} \dot{f} = -\lambda_0^* |s_0|^{\frac{2}{3}} sign(s_0) + z_1 \\ \ddot{f} = -\lambda_1^* |s_1|^{\frac{1}{2}} sign(s_1) - \lambda_2^* \int_0^t sign(s_1)\, dt \end{cases} \quad (10)$$

Proof: Let $\sigma_0 = s_0 - f$. With this change of coordinate, the two first equations of the system (7) can be written as follows:

$$\dot{\sigma}_0 = -\hat{\lambda}_0 |\sigma_0|^{\frac{2}{3}} sign(\sigma_0) - K_0 \sigma_0 + \sigma_1 \quad (11)$$

Where $\sigma_1 = z_1 - \dot{f}$.

Since $\hat{\lambda}_0 \geq 0$ and $K_0 > 0$, from (11) we have: $\sigma_1 - \dot{\sigma}_0 = sign(\sigma_0) \left[\hat{\lambda}_0 |\sigma_0|^{\frac{2}{3}} + K_0 |\sigma_0| \right]$ and we can conclude that:

$$sign(\sigma_1 - \dot{\sigma}_0) = sign(\sigma_0) \quad (12)$$

Subtracting $\dot{f}$ on both sides of the 2nd equation of (7), so we obtain:

$$v_0 - \dot{f} = -\hat{\lambda}_0 |\sigma_0|^{\frac{2}{3}} sign(\sigma_0) - K_0 \sigma_0 + z_1 - \dot{f} \quad (13)$$

Substituting $\dot{f}$ by its expression (10) in (13), we have:

$$\dot{\sigma}_0 = -\tilde{\lambda}_0 |\sigma_0|^{\frac{2}{3}} sign(\sigma_0) - K_0 \sigma_0 \quad (14)$$

with $\tilde{\lambda}_0 = \hat{\lambda}_0 - \lambda_0^*$, which is an error between the dynamic value of the gain and a priori one.

Considering now $\sigma_1 = z_1 - \dot{f}$, it gives $s_1 = \sigma_1 - \dot{\sigma}_0$. By subtracting $\ddot{f}$ from both sides of the last equation (7) and taking into account this change of variable, we have:

$$\dot{\sigma}_1 = -\tilde{\lambda}_1 |\sigma_1 - \dot{\sigma}_0|^{\frac{1}{2}} sign(\sigma_1 - \dot{\sigma}_0) - K_0 (\sigma_1 - \dot{\sigma}_0) - \tilde{\lambda}_2 \int_0^t sign(\sigma_1 - \dot{\sigma}_0)\, dt \quad (15)$$

Let us define a Lyapunov function as:

$$V(\sigma_0, \sigma_1, \tilde{\lambda}_i) = \frac{1}{2}\sigma_0^2 + \frac{1}{2}(\sigma_1 - \dot{\sigma}_0)^2 + \frac{1}{2}\sum_{i=0}^{2} \tilde{\lambda}_i^2, \;\; i \in \{0,1,2\} \quad (16)$$

The equilibrium point is defined by $X_e^{\sigma,\tilde{\lambda}} = (0,0,0)$. The derivative of this Lyapunov function is given by:

$$\dot{V} = \sigma_0 \dot{\sigma}_0 + (\sigma_1 - \dot{\sigma}_0)(\dot{\sigma}_1 - \ddot{\sigma}_0) + \tilde{\lambda}_0 \dot{\tilde{\lambda}}_0 + \tilde{\lambda}_1 \dot{\tilde{\lambda}}_1 + \tilde{\lambda}_2 \dot{\tilde{\lambda}}_2 \quad (17)$$

then

$$\sigma_0 \dot{\sigma}_0 + \tilde{\lambda}_0 \dot{\tilde{\lambda}}_0 = -K_0 \sigma_0^2 \quad (18)$$

and

$$(\sigma_1 - \dot{\sigma}_0)\dot{\sigma}_1 + \tilde{\lambda}_1 \dot{\tilde{\lambda}}_1 + \tilde{\lambda}_2 \dot{\tilde{\lambda}}_2 = -K_1 (\sigma_1 - \dot{\sigma}_0)^2 \quad (19)$$

Substituting (18) and (19) in (17):

$$\dot{V} = -K_0 \sigma_0^2 - K_1 (\sigma_1 - \dot{\sigma}_0)^2 - (\sigma_1 - \dot{\sigma}_0)\ddot{\sigma}_0 \quad (20)$$

We have,

$$-(\sigma_1 - \dot{\sigma}_0)\ddot{\sigma}_0 = -(\sigma_1 - \dot{\sigma}_0)\left[-\dot{\tilde{\lambda}}_0 |\sigma_0|^{\frac{2}{3}} sign(\sigma_0) - K_0 \dot{\sigma}_0 - \frac{2}{3}\tilde{\lambda}_0 |\sigma_0|^{-\frac{1}{3}} \dot{\sigma}_0 \right] \quad (21)$$

By introducing the dynamic gain $\hat{\lambda}_0$ (see system (9)) in (21), the following equality is satisfied:

$$-(\sigma_1 - \dot{\sigma}_0)\ddot{\sigma}_0 = -|\sigma_1 - \dot{\sigma}_0| \left[-|\sigma_0|^{\frac{7}{3}} + K_0^2 |\sigma_0| + \frac{2}{3}\tilde{\lambda}_0^2 |\sigma_0|^{\frac{1}{3}} + \frac{5}{3}\tilde{\lambda}_0 K_0 |\sigma_0|^{\frac{2}{3}} \right] \quad (22)$$

Consequently, the equation (17) can be rewritten as follows:

$$\dot{V} = -K_0 \sigma_0^2 - K_1 (\sigma_1 - \dot{\sigma}_0)^2 - \frac{2}{3}|\sigma_1 - \dot{\sigma}_0| \tilde{\lambda}_0^2 |\sigma_0|^{\frac{1}{3}} - |\sigma_1 - \dot{\sigma}_0| \left[-|\sigma_0|^{\frac{7}{3}} + \frac{5}{3}\tilde{\lambda}_0 K_0 |\sigma_0|^{\frac{2}{3}} + K_0^2 |\sigma_0| \right] \quad (23)$$

To show that $\dot{V}$ is negative, it is sufficient to prove that:

$$\Upsilon = \left[-|\sigma_0|^{\frac{7}{3}} + \frac{5}{3}\tilde{\lambda}_0 K_0 |\sigma_0|^{\frac{2}{3}} + K_0^2 |\sigma_0| \right] \geq 0 \qquad (24)$$

Therefore, let us assume that $|\tilde{\lambda}_0| \leq \tilde{\lambda}_{0M}$, where $\tilde{\lambda}_{0M}$ is a positive constant satisfying the following inequality:

$$\tilde{\lambda}_{0M} < \frac{3}{5} K_0 |\sigma_0|^{\frac{1}{3}} \qquad (25)$$

In order to obtain the condition defined by (24), one must choose K_0 such that:

$$K_0 \left[\tilde{\lambda}_0 + \frac{3}{5} K_0 |\sigma_0|^{\frac{1}{3}} \right] \geq \frac{3}{5} |\sigma_0|^{\frac{5}{3}} \qquad (26)$$

It is obvious that it is always possible to find some value of K_0 (namely a high-value) satisfying both inequalities (24) and (25).

Then, we can conclude that $\dot{V}$ is a negative function $\forall (\sigma_0, \sigma_1, \tilde{\lambda}_i) \in \mathbb{R}^3$ but this property vanishes for $(\sigma_0 = 0, \sigma_1 = 0, \tilde{\lambda}_i)^T \neq X_e^{\sigma,\tilde{\lambda}}$. So, $\dot{V}$ is a globally semi-negative definite function on $\mathbb{R}^3$ and it is defined a locally negative definite function on $\mathbb{R}^3 \left| (\sigma_0 = 0, \sigma_1 = 0, \tilde{\lambda}_i)^T \right.$. Consequently, this Lyapunov function proves a global convergence on $\mathbb{R}^3$ of the equilibrium point. This means also that a local asymptotic convergence of the algorithm has been proven on. Even with using the LaSalle's invariance principle, the global asymptotic convergence of the system equilibrium point is cannot be shown.

Remark: The given proof does not guarantee the convergence of dynamic gains to λ_0^* and λ_1^*. Furthermore, these dynamic gains change over time according to the imposed adaptation laws. With corresponding to the equations of dynamic gains, they will evolve continuously. Then, to avoid saturation on these gains is imposed. In all tests carried out, the dynamic gains have a bounded evolution depending on the initial values of the algorithm gains.

3. ELECTROPNEUMATIC SYSTEM MODEL

The electropneumatic system (see figure 2) is a linear inline double acting servo-drive using a single rod with a stroke equal to 500 mm. It is controlled by two servo-distributors and is composed by two chambers denoted *P* and *N*. The air mass flow rates *qm* entering in the chambers are modulated by two three-way servo-distributors. The actuator rod is connected to one side of the carriage and drives an inertial load on guiding rails. The total mass (piston, rod and carriage) is equal to 17 kg. The considered system model can be got using some physical laws: the fundamental mechanical equation, the mass flow rate through a restriction and the pressure behaviour in a chamber with variable volume. Each chamber of the actuator is considered as a variable volume which is obtained assuming the classical following assumptions [11]:

A1. Air is a perfect gas and its kinetic energy is inconsequential.

A2. The pressure and the temperature are homogeneous in each chamber.

A3. The process is polytropic and characterized by coefficient k.

Thus, the combination of all previous assumptions and considering that the temperature variation is negligible with respect to average and equal to the supply temperature, the electropneumatic system model is then obtained. The bandwidth of actuator is ten times greater than the servo-distributor bandwidth. Then its dynamics can be neglected and its model can be reduced to a static one described by two mass flow rates $q_m^P(u_P, p_P)$ and $q_m^N(u_N, p_N)$. These last one depend on the input voltages u_P, u_N and the output pressures p_P, p_N.

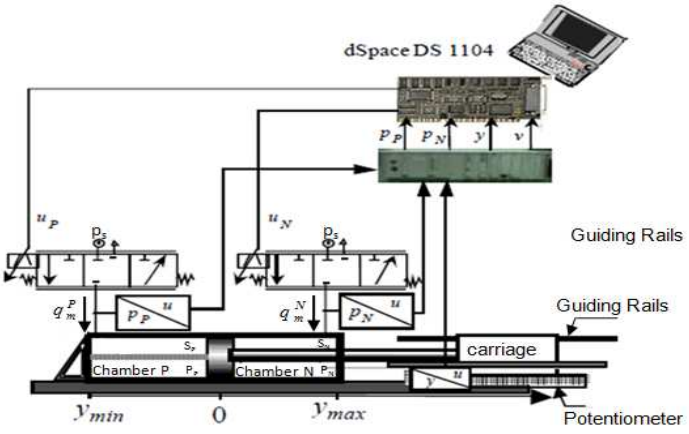

Figure 3. Electropneumatic system.

The model equations are given by the following system which is developed to get a simplest one which allows the design of control law:

$$\begin{cases} \dfrac{dy}{dt} = v \\ \dfrac{dv}{dt} = \dfrac{1}{M}\left[S_P p_P - S_N p_N - bv - F_{ext} \right] \\ \dfrac{dp_P}{dt} = \dfrac{krT}{V_P(y)}\left[q_m^P(u_P, p_P) - \dfrac{S_P}{rT} p_P v \right] \\ \dfrac{dp_N}{dt} = \dfrac{krT}{V_N(y)}\left[q_m^N(u_N, p_N) + \dfrac{S_N}{rT} p_N v \right] \end{cases} \qquad (27)$$

Where: $\begin{cases} V_P(y) = V_P(0) + S_P y \\ V_N(y) = V_N(0) - S_N y \end{cases}$ and with:

$\begin{cases} V_p(0) = V_{DP} + S_P \dfrac{l}{2} \\ V_N(0) = V_{DN} + S_N \dfrac{l}{2} \end{cases}$ are the piping volumes of the chambers

for the zero position and V_{DP}, V_{DN} are dead volumes present at each extremities of the cylinder. In the mechanical equation, F_{ext} represents an external constant force due to atmospheric pressure and bv is the viscous friction.

The used test bench operates with two three-way proportional servo-distributors. With the opposite signs of the input $(u_P = u)$ and $(u_N = -u)$, it is possible to suppose that these two servo-distributors are equivalent to the one five-way proportional servo-distributor, [9]. So the two servo-distributors are assumed that are identical and symmetrical.

In order to establish a mathematical model of the power modulator flow stage, many research works present approximations based on physical laws [12] by modelling of the geometrical variations of the restriction areas of the servo-distributor, as well as by experimental characterization [13].

In this paper, the models of the mass flow rates q_m^P and q_m^N are issue of empirical method, [14]. With these experimental measures, the global characterization corresponds to the static measurement of the output mass flow rate q_m, which depends on the input control u and the output pressure p, for constant source and the exhaust pressure. Hence, this global characterization has the advantage of obtaining simply, by projection of the characteristic series $q_m(u,p)$ on three planes: (p,q_m), (u,q_m) and (u,p). The authors in [15] have developed analytical models for both simulation and control purposes.

Then, the flow stage characteristics were approximated by polynomial functions affine in control such that:

$$q_m(u,p) = \phi(p) + \psi(p, sign(u)). \quad (28)$$

Where $\phi(.)$ represents the mass flow rate leakage (see figure 4 (a)). The function $\psi(.)$ represent the mass flow rate characteristic which is a positive quantity over the physical domain and its evolution is described for both inlet $(u > 0)$ and exhaust $(u < 0)$ case (see figure 4(b)).

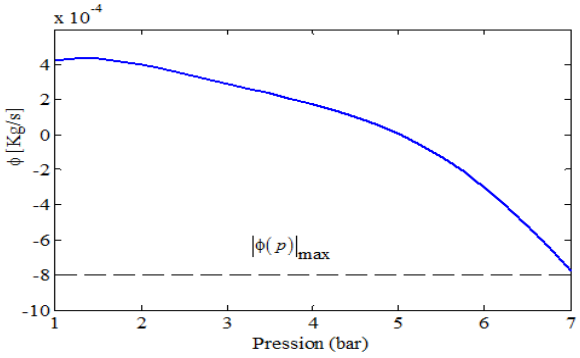

(a) Evolution of the function $\phi(p)$.

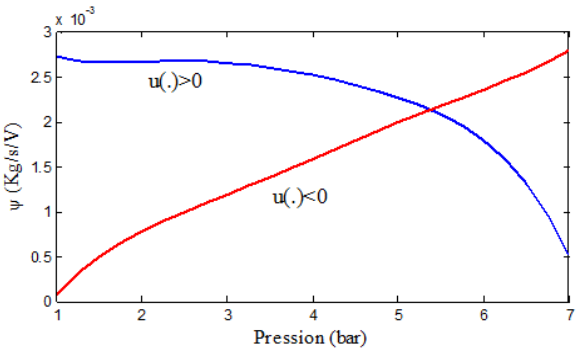

(b) Evolution of the function $\psi(p)$.

Figure 4. Evolution of the functions describing the polynomial characteristic of the mass flow rate.

Using (27) and (28), the nonlinear affine model with a single-input is given by:

$$\dot{x} = f(x) + g(x).u \quad (29)$$

with $x, f(x), g(x) \in \mathbb{R}^4$ and $u \in \mathbb{R}$, where: $x = [y, v, p_P, p_N]^T$,

$$f(x) = \begin{pmatrix} v \\ \frac{1}{M}\left[S_P p_P - S_N p_N - bv - F_{ext}\right] \\ \frac{krT}{V_P(y)}\left[\phi(p_P) - \frac{S_P}{rT} p_P v\right] \\ \frac{krT}{V_N(y)}\left[\phi(p_N) + \frac{S_N}{rT} p_N v\right] \end{pmatrix},$$

$$g(x) = \begin{pmatrix} 0 \\ 0 \\ \frac{k.r.T}{V_P(y)}.\psi\left(p_P, \mathrm{sgn}(u)\right) \\ -\frac{k.r.T}{V_N(y)}.\psi\left(p_N, \mathrm{sgn}(-u)\right) \end{pmatrix}$$

4. Effectiveness of Proposed Differentiator Against Measurement Noise

In order to consider the effectiveness of the PD in real time process with the presence of measurement noises, the algorithm is tested on the electropneumatic test bench. The position is measured, while the actuator is tracking a sinusoidal signal as a reference input with a fixed gain linear controller. The sampling frequency of the control loop is equal to 1 kHz. The electropneumatic position of the actuator is measured by a potentiometer position having 500mm as measurement range and a 40mV/mm as sensitivity. The measured position is then applied as input to the differentiator, which aims to estimate velocity and acceleration of the actuator.

For this comparative study, let choice the Classic Backward Differentiation (CBD) algorithm. In CBD a double value of sampling time T_e is considered as:

$$output(k) = \frac{input(k) - input(k-2)}{2T_e} \quad (30)$$

In order to compare the algorithm CBD defined by (30) to those based on the higher order sliding modes (RD, PD), a sinusoidal signal which applied to the position of the actuator is chosen as follows: $f(t) = A.\sin(2.\Pi.f_{req}.t)$, where $f_{req} = 1Hz$ and $A = 0.1m$. Figure 5 presents the actuator position given by the potentiometer. It is clear that the obtained position is not exactly a sinusoidal signal. This is due to the presence of some nonlinearity in the model system which is not compensated by the used controller. For this test, the accuracy of tracking is not a main priority. That is the reason why the maximum amplitude of the measured position (see figure 5) does not attain the imposed value.

The outputs of different differentiators are reproduced by the following figures. The cut-off frequency of the PD is tuned by the couple gain (K_0 , K_1) in order to have: $f_c \geq 2f_{dyn}$, where f_{dyn} is the natural frequency estimated for the system. For the electropneumatic system, this frequency is equal to 2Hz around a central position.

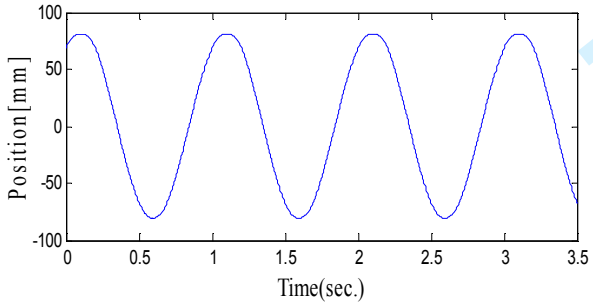

Figure 5. Measured position [mm].

From figures 6, 7 and 8, the estimated velocity given by the different algorithm are compared to the output of the velocity sensor which is implemented on our test bench. This sensor is based on a magnetostrictive technology and it has 5V/m.s^{-1} as sensitivity. It is noteworthy that for approximately the same bandwidth the estimation of the outputs obtained with the PD is less noisy than RD and CDB, especially for the estimation of the acceleration (see figures 9, 10 and 11). To improve the signal output of the RD, it is necessary to find the best gains to have a compromise between the exactitude and the level of noise for the considered signal. In order to estimate the acceleration with the CDB, the output of a velocity sensor is used as an input to the CDB.

We do not have an accelerometer implemented at the bench trial, so we just presented the estimated accelerations, in order to show just the robustness against the measurement noise of the different algorithm. Figure 8 shows that the PD is insensitive to high frequency components of the position signal while the output of the RD consists of the accurate derivative and some high frequency noise. Moreover, it can be seen that the algorithms based on the high sliding modes presents better results than the CDB algorithm.

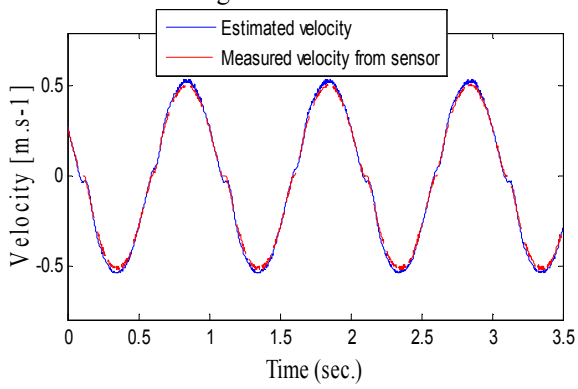

Figure 6. Velocity [m.s-1] estimated by PD.

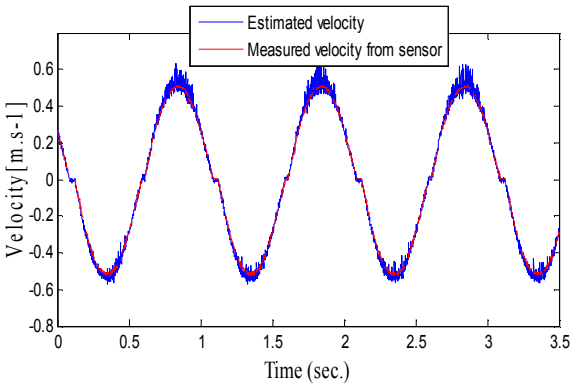

Figure 7. Velocity [m.s-1] estimated by RD.

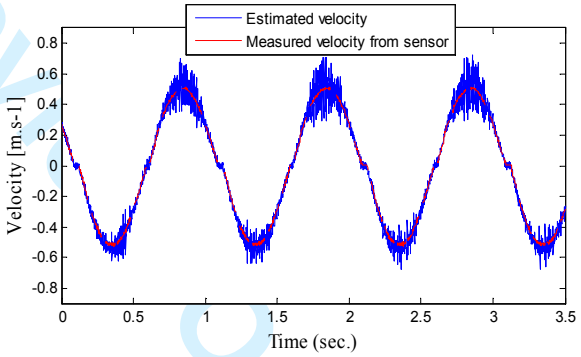

Figure 8. Velocity [m.s-1]: estimated by CDB.

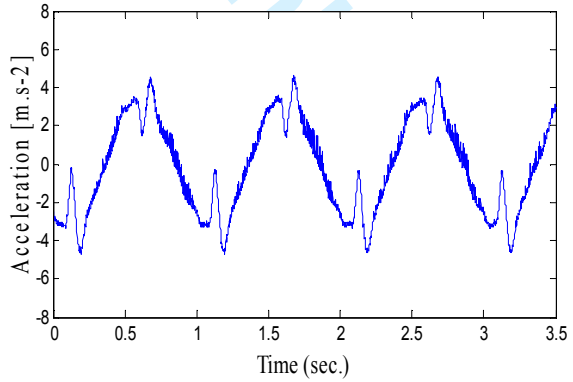

Figure 9. Acceleration [m.s-2] estimated by PD.

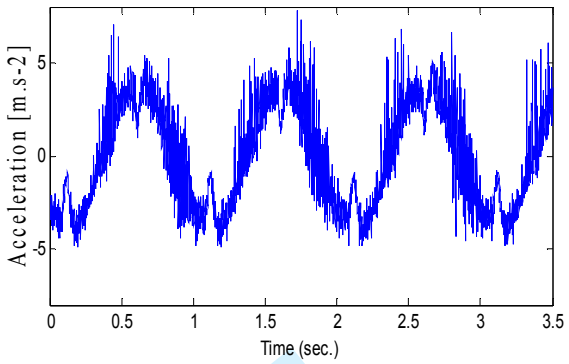

Figure 10. Acceleration [m.s-2] estimated by RD.

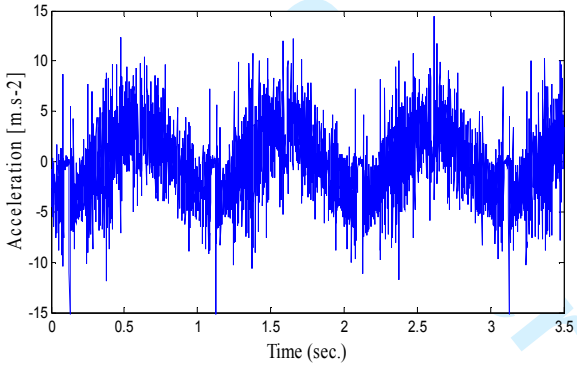

Figure 11. Acceleration [m.s-2] estimated by CDB.

5. Effectiveness of Proposed Differentiator Design In Control

In this section, a comparative study between the two algorithms (PD and CBD) and their influence on the control law of the electropneumatic system are presented. The comparative study with the CBD is an interesting one because such algorithm is widely used in different applications and especially an industrial one. See [17], for the comparative study between (RD, PD) applied to the high dynamic electro-hydraulic system where it is possible to have high-frequency signals.

Now, for this target and using the electropneumatic model (29), a classic simple control strategy is synthesized. This one consists to use the point to point tracking which the controller must ensure a good static accuracy. This controller is based on the local linearization of the nonlinear dynamics system around a nominal operating point [11]. For the linearized model [11], two assumptions must be considered:

A4. the actuator is symmetrical,

A5. external constant force is zero.

These assumptions can be deduced from the equal pressure in both chambers, at equilibrium state. The state feedback control law u can be given by:

$$u = u^e + K_y(y - y_r) + K_v v + K_a a \qquad (31)$$

with K_y, K_v, K_a are respectively a feedback-gains of position, velocity and acceleration. y_r is a reference input signal. The coefficients of (31) are setting in order to obtain the dynamics of the closed loop system as a canonical Brunovsky form [13].

Experimental results are performed on the test bed presented in Section III. The sampling frequency of the control loop is equal to 1 kHz. Control law given by (31) is implemented using a Dspace 1104 controller board with the dedicated digital signal processor. The sensed signals, all analog were run through the signal conditioning unit before being read by the A/D converter. The position is given by an analog potentiometer. The control law is implemented with using two sensors. Indeed, the position sensor is a NovoTECHNIK model TLH500, which has a precision equal to 10µm. The experimental validation consists to compare the efficiency of the CDB design in controller target to the PD. Then, a square signal is chosen as a reference signal position, with the displacement magnitude equal to 40% of the total stroke around the central position.

Firstly, the classic algorithm (30) is used to recover the velocity and the acceleration. From the measured position, the velocity is building. By using the cascade form of classic algorithm, the acceleration is estimated (see figure 14). The control input (see figure 15) is affected by the chattering phenomenon, which is due to the velocity and mostly to the acceleration signal (see figures 13 and 14). By zooming figure 12, it turned out that the maximum static error of position is equal to 1.15mm, which is about 0.575% of the total displacement magnitude.

Now, the PD is used to recover the velocity and the acceleration signal. With using this algorithm, we find relatively the same form of the signal given in figure 12. However, the maximum static position error is equal to 0.14mm, which is about 0.28% of the total displacement magnitude.

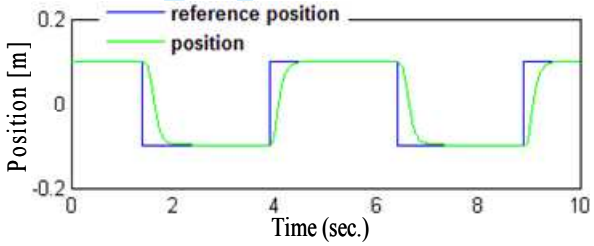

Figure 12. Position and Reference position [m]: with DA.

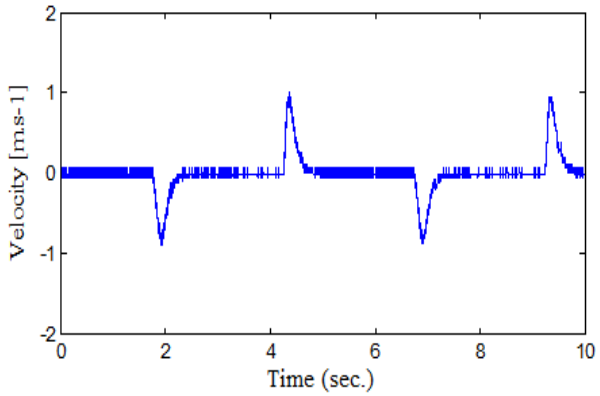

Figure 13. Velocity [m.s-1]: with CDB.

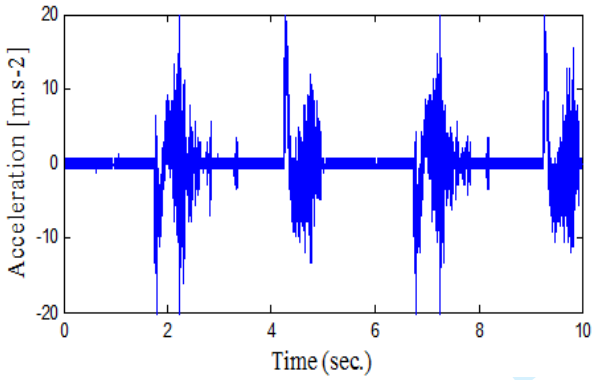

Figure 14. Acceleration [m.s-2]: with CDB.

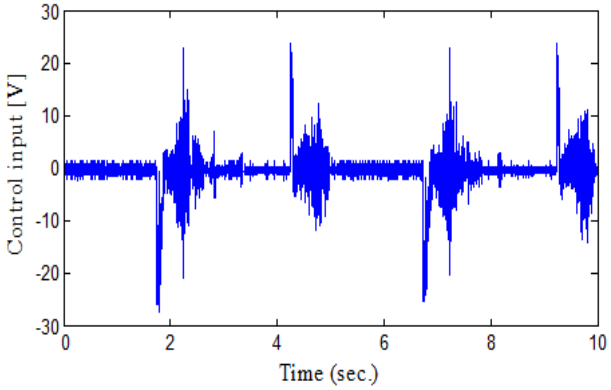

Figure 15. Control input [V]: with CDB.

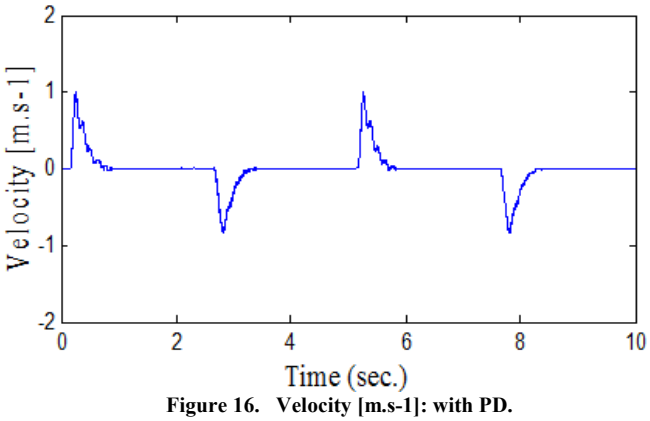

Figure 16. Velocity [m.s-1]: with PD.

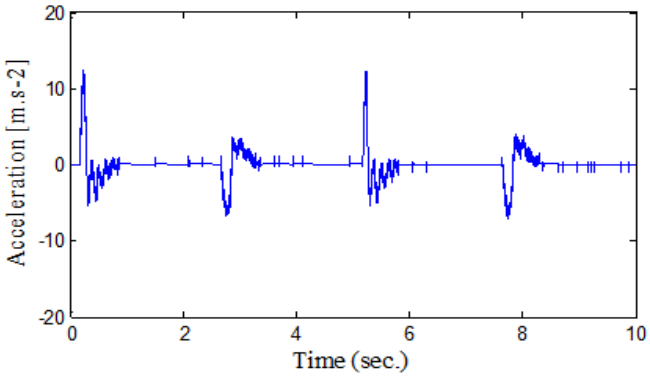

Figure 17. Acceleration [m.s-2]: with PD.

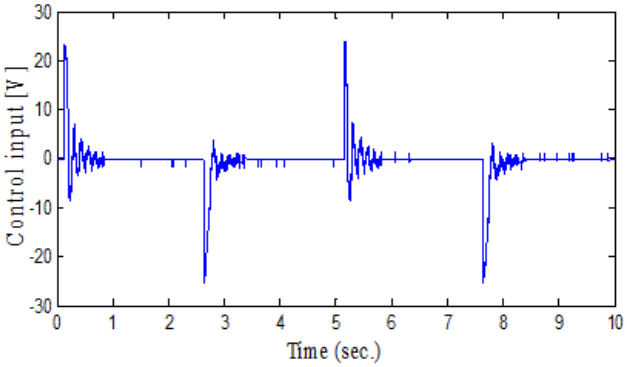

Figure 18. Control input [V]: with PD.

Remark that this value is smaller than twice compared to the classic algorithm. Considering figure 18, the control signal is smooth, which is a good property from an energetically efficient point of view. Therefore the smooth control seems to provide a more satisfactory lifetime of components. This smoothness is due to the estimated velocity and acceleration signal (see figures 16 and 17).This is due to the dynamic laws added to the classic robust differentiator, which allows emphasizing the convergence of estimation error in real time. In such case, the error between the accurate and the estimated signal is minimized. Therefore, the dynamic gains improve the signal filtration by carefully choosing the gains K_0 and K_1 comparing to the bandwidth of the system.

6. CONCLUSION

In this paper, a novel form of the 2nd-order robust dynamic differentiator has been proposed to overcome the problem of the tuning gains of sliding mode differentiator. The direct validation highlights the performances of the proposed algorithm. Experimental results are carried out in order to show the importance of the choice differentiator design on the control of an electropneumatic system. The proposed algorithm shows a satisfactory result compared to some other classic differentiators. The algorithm efficiently attenuates the noise for these two outputs. This improvement allows reducing the noise in the control input and the reduction of chattering effect, in order to increase the tracking performance in term of point-to-point tracking.

Several perspectives could be considered for the future. For example, the effectiveness of the proposed algorithm could be tested for other different types of process. Theoretical perspective is to prove the overall convergence system combining the differentiator with the control loop.

REFERENCES

1. V. Alfieri, G. Conte, C. Pedicini, "Feedback linearization control for the air & charging system in a diesel engine", *European Control Conf.*, 2015, Linz, Austria
2. A. Ayadi, S. Hajji, M.Smaoui, and A. Chaari, Adaptive Moving Sliding Mode Control for SISO Systems: Application to an Electropneumatic System, *J. of Control Science and Engineering*, Vol. 2016, p.10.
3. V. Wowk, Machinery Vibration, Measurement and Analysis. New York: McGraw-Hill, 1991. R. Haipeng and F. Juntao, Adaptive Backstepping Slide Mode Control of Pneumatic Position Servo System, Chinese J. of Mechanical Engineering, Vol. 29(5), 2016, pp. 1003-1009.
4. R. Abd. Rahman, L. He, N. Sepehri, "Design and experimental study of a dynamical adaptive backstepping–sliding mode control scheme for position tracking and regulating of a low-cost pneumatic cylinder", *Inter. J. of Robust and Nonlinear Control*, Vol. 26(4), 2016, pp. 853–875.
5. Y. Shtessel, F. Plestan, M.Taleb, "Super-twisting adaptive sliding mode control with not-overestimated gains: application to an electropneumatic actuator", *IFAC World Congress*, 2011, pp.1-11.
6. V. Utkin. Sliding mode control in electromechanical systems, Taylor & Francis, 1999.
7. A. Levant. "Robust exact differentiation via sliding mode technique", *Automatica*, Vol. 34, pp. 379-384, 1998.
8. M. Smaoui, X. Brun, and D. Thomasset, "A robust differentiator-controller design for an electropneumatic system", *Proceeding of the 44th IEEE Conf. on Decision and Control and the European Control Conf.*, 2005, Sevilia, Spain.
9. A. Levant. Higher order sliding modes,"Ddifferentiation and output feedback control", *Inter. J. of Control*, Vol.76, pp. 924-941, 2003.
10. J-P. Barbot , A. Levant , M. Livne, D. Lunz, "Discrete Sliding-Mode-Based Differentiators", *14th Inter. VSS Workshop*, 2016, Nanjing, China.
11. J.L. Shearer, "Study of pneumatic processes in the continuous control of motion with compressed air", *Parts I and II. Transaction of the American Society of Mechanical Engineers*, Vol. 78, pp. 233-249, 1956.
12. K. Araki. "Effects of valve configuration on a pneumatic servo", *International Fluid Power Symposium*, pp. 271-290, 1981.
13. E. Richard and S. Scavarda, "Comparison between linear and nonlinear control of an electropneumatic servodrive", *J. of Dynamic Systems, Measurement, and Control*, Vol. 118, pp. 245-252, 1996.
14. S. Sesmat and S. Scavarda. "Static characteristics of a three way servovalve", *Proceeding of the 12th Aachen Conf. on Fluid Power Technology*, 1996, Aachen, Germany, pp. 643-652.
15. M. Belgharbi, D. Thomasset, S. Scavarda and S. Sesmat. "Analytical model of the flow stage of a pneumatic servodistributor for simulation and nonlinear control", *6th Scandinavian Inter. Conf. on Fluid. Power*, 1996, Tampere, Finland, pp.847-860.
16. L. Sidhom, X. Brun, M. Smaoui, E. Bideaux, and D. Thomasset, "Dynamic gains differentiator for hydraulic system control", *J. of Dynamic Systems, Measurement and Control*, Vol. 137, No. 4, 2015.
17. V. Chawda, O. Celik, MK. O'Malley,"Application of Levant's Differentiator for Velocity Estimation and Increased Z-Width in Haptic Interfaces", *IEEE World Haptics Conf.,*Istanbul, Turkey, 2011.
18. M.T. Angulo, J.A. Moreno, L. Fridman, "The differentiation error of noisy signals using the Generalized Super-Twisting differentiator", *51st IEEE Conf. on Decision and Control*, Maui, Hawaii, 2012.
19. S. Väliviita, S. J. Ovaska, "Delayless acceleration measurement method for elevator control", *IEEE Trans. Ind. Electron.* Vol. 45, No. 2, pp. 364-366, 1998.
20. J. Zhang, A. K. Swain, S. K. Nguang, Robust Sliding Mode Observer based Fault Estimation for Certain Class of Uncertain Nonlinear Systems, *Asian J. of Control*, Vol. 17(4), 2015, pp. 1296-1309.
21. J. Davila, L. Fridman, A. Pisanob and E. Usaib. Finite-time state observation for non-linear uncertain systems via higher-order sliding modes, Int. J. of Control, 2009, Vol. 82, No. 8, pp. 1564-1574.
22. F. Courreges, "Design of a discrete algebraic robust differentiation FIR filter using an annihilator of the Z-transform; frequency response analysis and parameter tuning", *Numerical Algorithms*, Vol. 68(4), 2015, pp. 867-901
23. M. Mboup, C. Join, M. Fliess, "Numerical differentiation with annihilators in noisy environnement", *Numerical Algorithms*, Vol. 50, No. 4, pp. 439-467, 2009.

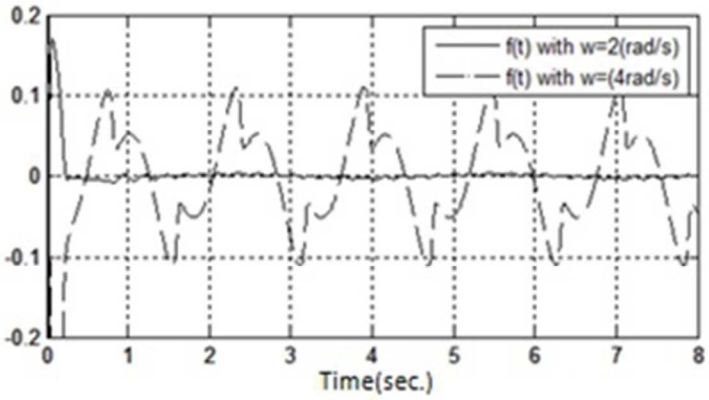

Figure 1. Error evolution for the 1st derivative estimate.

94x53mm (96 x 96 DPI)

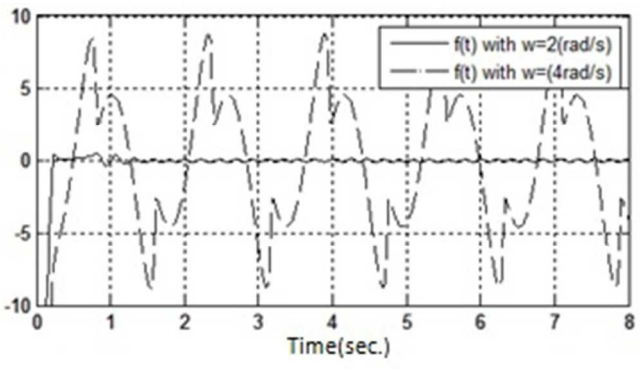

Figure 2. Error evolution for the 2nd derivative estimate.

88x48mm (96 x 96 DPI)

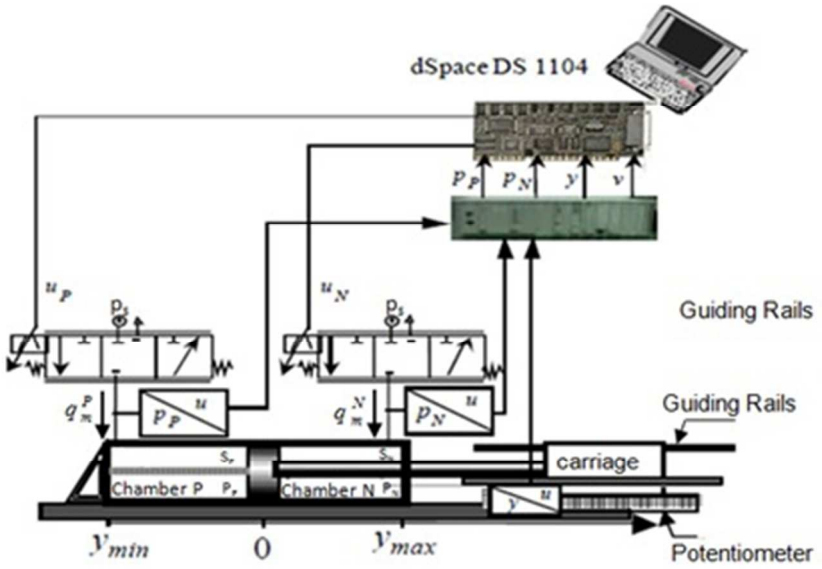

Figure 3. Electropneumatic system.

110x78mm (96 x 96 DPI)

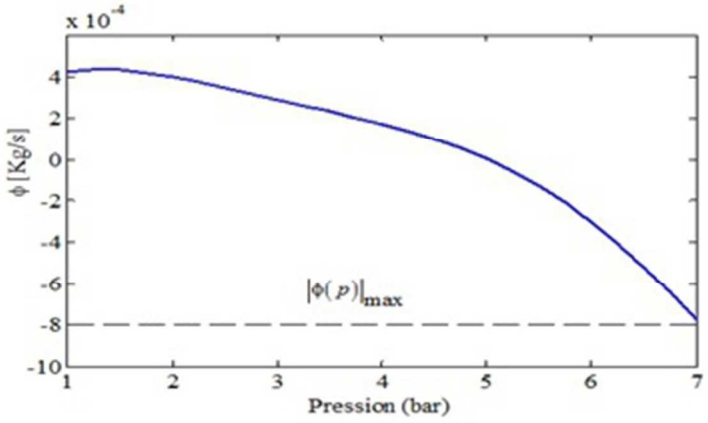

(a) Evolution of the function

95x57mm (96 x 96 DPI)

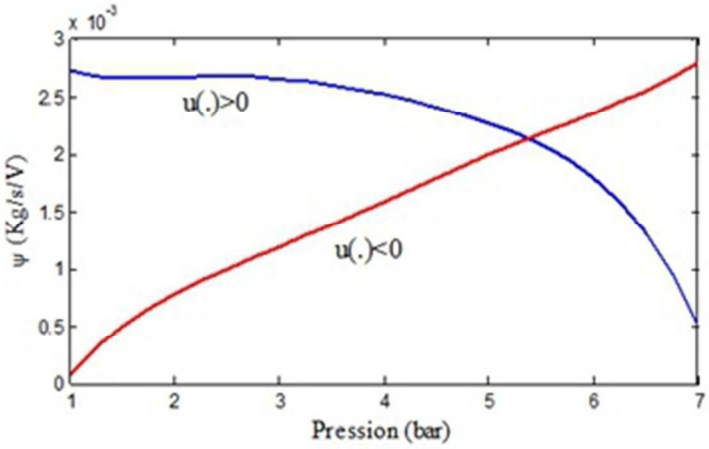

(b) Evolution of the function .

94x59mm (96 x 96 DPI)

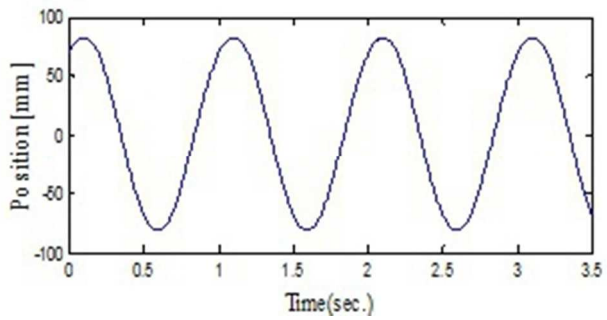

Figure 5. Measured position [mm].

84x42mm (96 x 96 DPI)

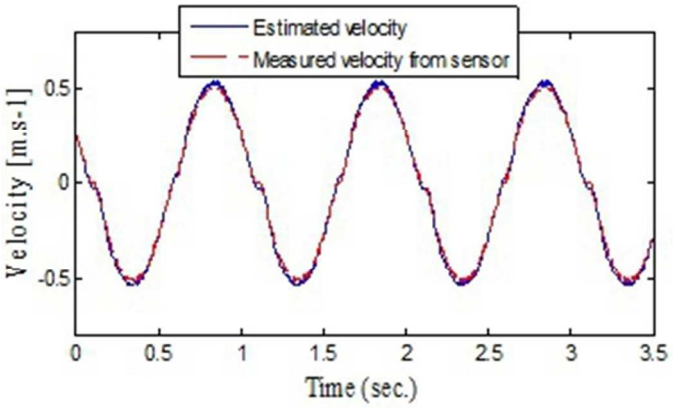

Figure 6. Velocity [m.s-1] estimated by PD.

89x54mm (96 x 96 DPI)

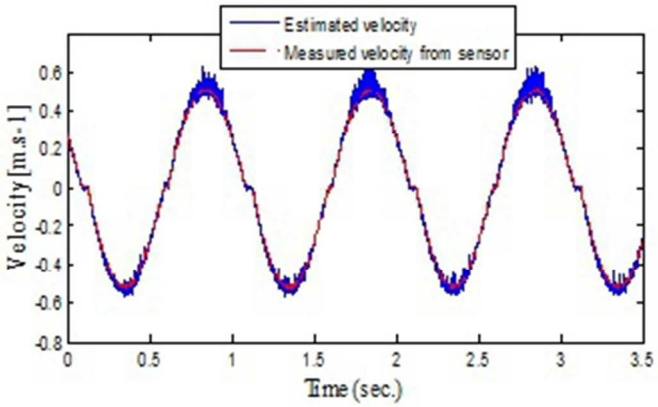

Figure 7. Velocity [m.s-1] estimated by RD.

87x54mm (96 x 96 DPI)

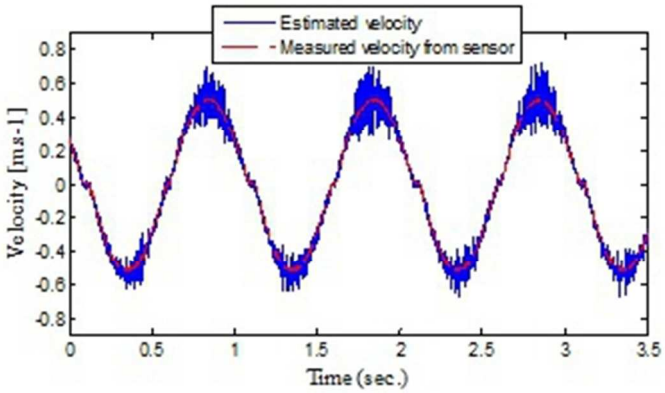

Figure 8. Velocity [m.s-1]: estimated by CDB.

89x52mm (96 x 96 DPI)

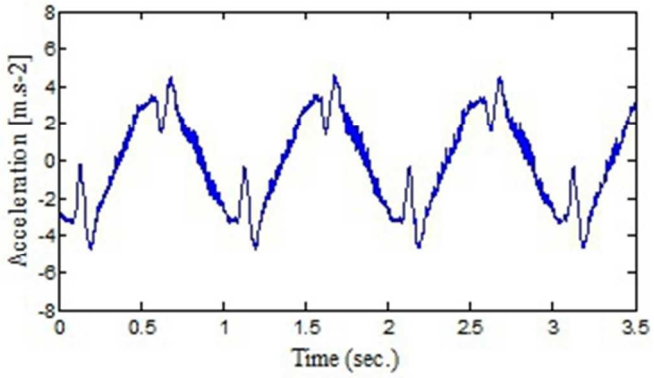

Figure 9. Acceleration [m.s-2] estimated by PD.

87x51mm (96 x 96 DPI)

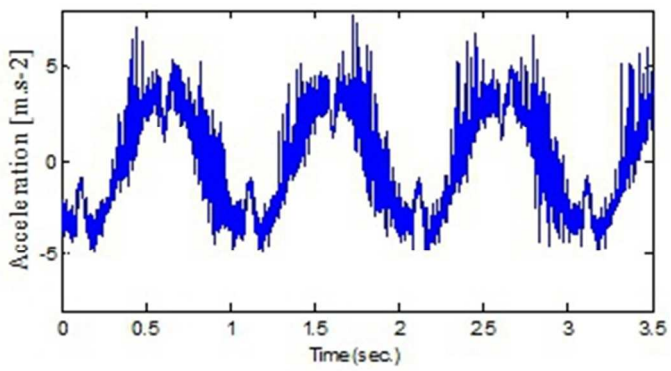

Figure 10. Acceleration [m.s-2] estimated by RD.

88x48mm (96 x 96 DPI)

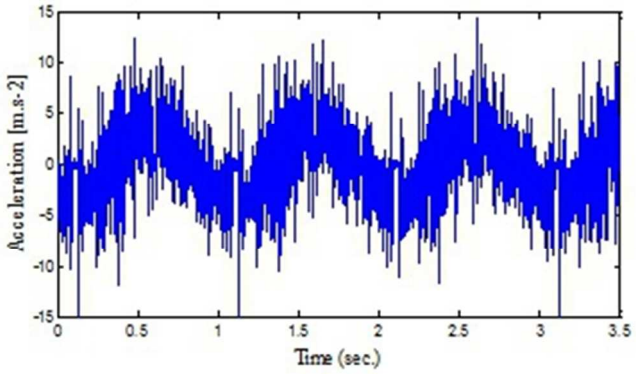

Figure 11. Acceleration [m.s-2] estimated by CDB.

84x49mm (96 x 96 DPI)

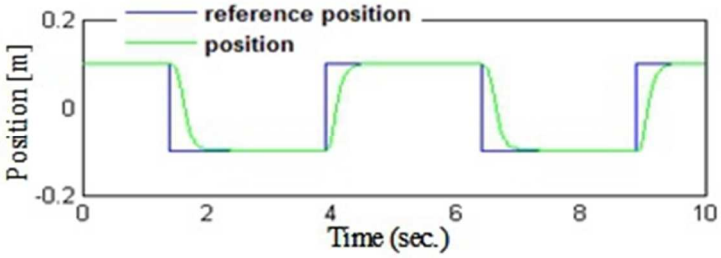

Figure 12. Position and Reference position [m]: with DA.

96x37mm (96 x 96 DPI)

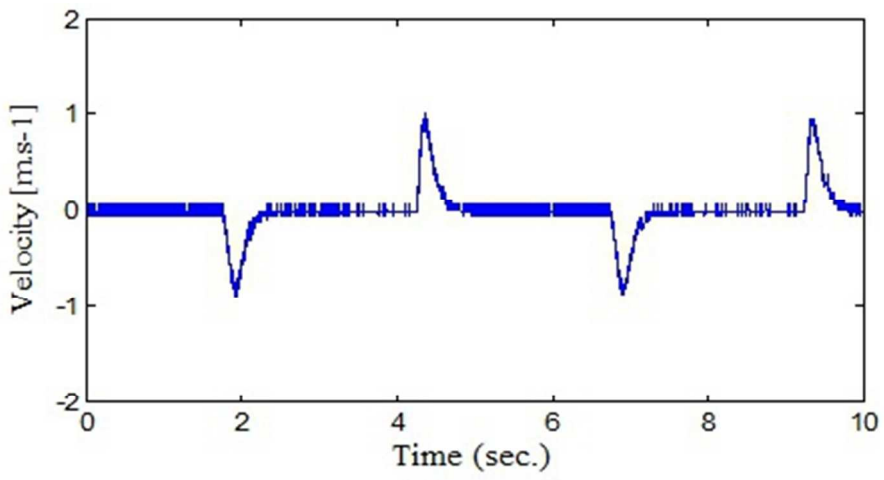

Figure 13. Velocity [m.s-1]: with CDB.

126x64mm (96 x 96 DPI)

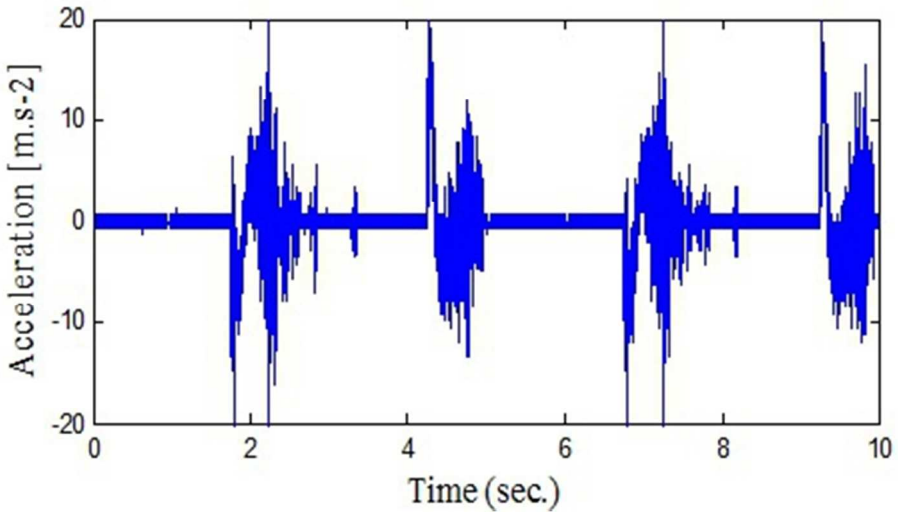

Figure 14. Acceleration [m.s-2]: with CDB.

123x67mm (96 x 96 DPI)

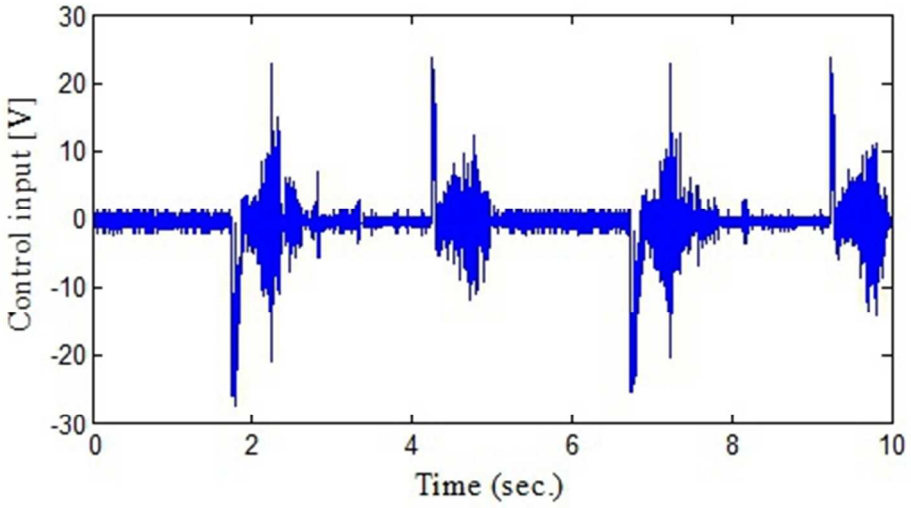

Figure 15. Control input [V]: with CDB.

123x67mm (96 x 96 DPI)

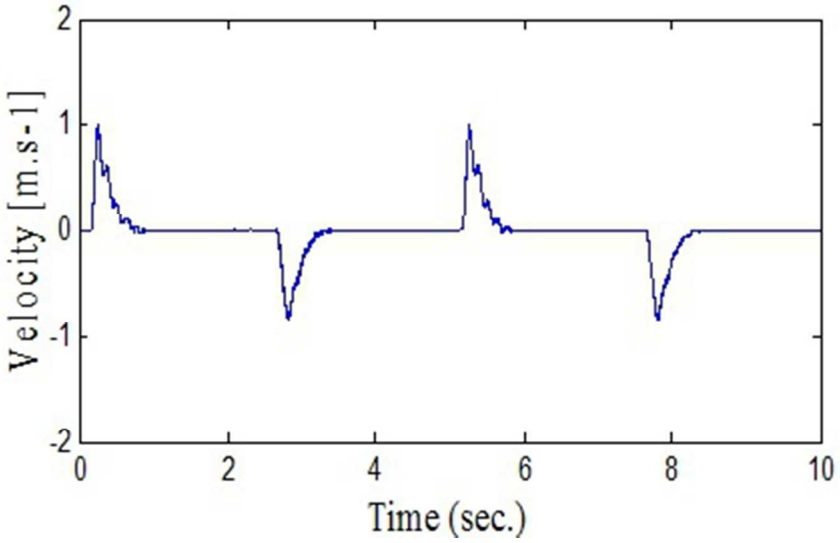

Figure 16. Velocity [m.s-1]: with PD.

115x71mm (96 x 96 DPI)

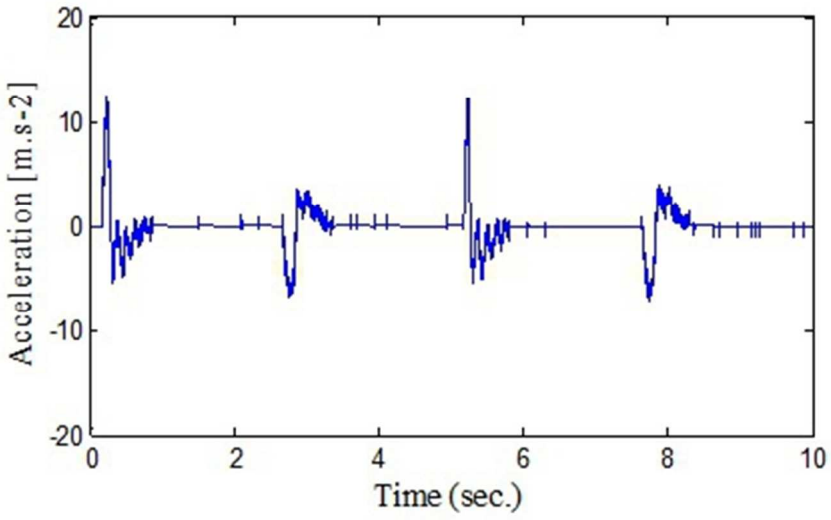

Figure 17. Acceleration [m.s-2]: with PD.

112x70mm (96 x 96 DPI)

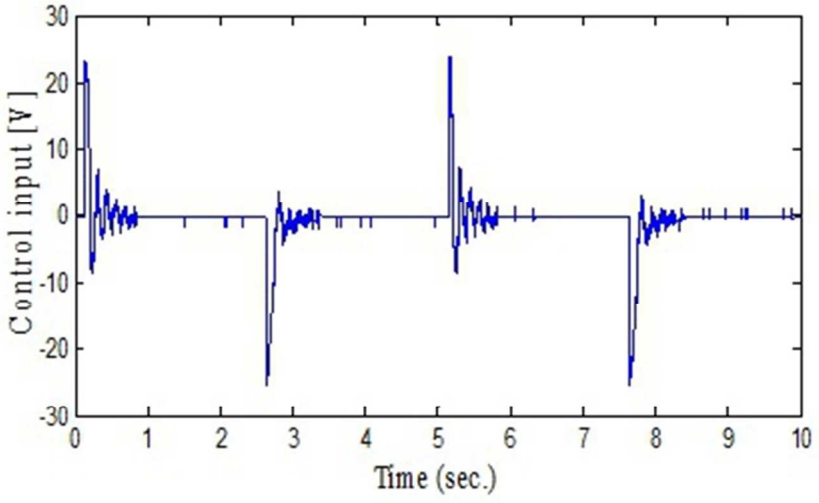

Figure 18. Control input [V]: with PD.

112x67mm (96 x 96 DPI)